

COMPUTATION OF \wp -FUNCTIONS ON PLANE ALGEBRAIC CURVES

J BERNATSKA

ABSTRACT. Numerical tools for computation of \wp -functions, also known as Kleinian or multiply periodic, are proposed. In this connection, computation of periods of the both first and second kind is reconsidered. An analytical approach to constructing the Riemann surface of a plane algebraic curves of low gonality is used. The approach is based on explicit radical solutions to quadratic, cubic, and quartic equations, which serve for hyperelliptic, trigonal, and tetragonal curves, respectively. The proposed analytical construction of the Riemann surface gives a full control over computation of the Abel image of any point on a curve. Therefore, computation of \wp -functions on given divisors can be done directly. An alternative computation with the help of the Jacobi inversion problem is used for verification. Hyperelliptic and trigonal curves are considered in detail, and illustrated by examples.

1. INTRODUCTION

The interest to computing \wp -functions, also known as Kleinian after [10], or multiply periodic after [3], arises from the realm of completely integrable systems, e.g. the hierarchies of the Korteweg—de Vries equation (KdV), sine-Gordon equation (SG), non-linear Schrödinger equation (NLS), etc., since finite-gap solutions can be expressed in terms of these functions, see [10, 6]. This representation of solutions is rarely used, and a convenient tools for computation are not developed.

The only numerical computation, and graphical representation, of solutions in terms of $\wp_{1,1}$ -function can be found in [22, 23], for the mKdV equation, and the KdV equation, respectively. Since solutions are required to be real-valued, $\wp_{1,1}$ -function is computed along a particular path in the Jacobian variety. Computation of periods on a curve is avoided. Instead, $\wp_{1,1}$ -function is expressed in terms of a divisor on a hyperelliptic curve, which follows from the Jacobi inversion problem. Solving the equation is reduced to computing the Abel map by means of Euler's numerical quadrature. The required path in the Jacobian variety is constructed numerically to satisfy the reality condition for the solution.

On the other hand, solutions of completely integrable equations in term of theta functions, see for example [4], are widely used. And numerical tools for computation of the Riemann period matrix and the theta function are well developed.

A powerful method of computing first kind period matrices (normalized and not normalized) on a plane curve was presented in [14], and implemented in the Maple package `algcurves`, see a detailed description in [15]. Besides this, other packages for computing the theta function and its derivatives are created in Sage, Matlab, Julia, see for example [1].

Date: July 9, 2024.

Computation with the help of spectral approximation is suggested in [19]. Linear combinations of Chebyshev polynomials are used in approximation of integrands of first and third kind integrals between branch points, and integration is performed with the help of the orthogonality relation on the polynomials. Numerical simulation is performed in Matlab. With Riemann period matrices computed by means of this technique, solutions of the KdV and KP equations on hyperelliptic curves of genera 2, 4, 6 were computed and illustrated in [20]. Solutions of the NLS equation and the Davey–Stewartson equation on hyperelliptic curves of genera 2 and 4 were presented in [21]. The spectral approximation technique allows to approach almost solitonic cases, when pairs of branch points collide.

The mentioned numerical tools are designed for studying theta-functional solutions. And appropriate and convenient numerical tools are needed for computation of \wp -functions, as well. First of all, periods of the both first and second kinds are required, the latter are not covered by the known packages. The necessary second kind differentials form an associate system with the standard first kind differentials. As a result, not normalized period matrices of the first and second kinds, subject to the Legendre relation, are obtained. Also a technique of computing the Abel map is needed for direct computation of \wp -functions.

In the present paper, an effective analytical method of direct computation on plane algebraic curves of low gonality is proposed. The method is based on constructing the Riemann surface of a curve from explicit solutions obtained as radical expressions for roots of a quadratic, cubic, or quartic equation, which serve for a hyperelliptic, trigonal, or tetragonal curve, respectively. Continuous connection between these solutions can be discovered analytically. Such an analytical construction of the Riemann surface gives a full understanding how to compute the Abel image of any point on the curve.

This analytical approach was initiated by V. Enolsky, and the hyperelliptic case with real branch points was developed by him. First and second kind periods obtained by this method served for verification of relations on theta functions, and \wp -functions. However, the method had never been published before. In the present paper the method is extended to hyperelliptic curves with arbitrary complex branch points, and to trigonal curves. These two types of plane algebraic curves are the most demanded. In fact, only integrable systems with hyperelliptic spectral curves are considered in the literature, when computation arises.

In addition to direct computation of \wp -functions, computation based on the Jacobi inversion problem is also presented. The latter is used for verification that obtained values of \wp -functions, as well as periods used for computing \wp -functions, serve for the curve in question. In the hyperelliptic case, generalizations of Bolza formulas, which give expressions for branch points in terms of theta functions with characteristics, are used for verification of computed periods.

The method is illustrated by examples: hyperelliptic curves of genus 4 with (1) complex branch points, and (2) all real branch points, and a trigonal curve of genus 3. All computations are made in Wolfram Mathematica.

2. PRELIMINARIES

2.1. Sato weight. The notion of *Sato weight* plays an important role in the theory of (n, s) -curves. Such a curve arises as a universal unfolding of the Pham singularity $y^n + x^s = 0$ with co-prime n and s , $n < s$. Thus, an (n, s) -curve is defined by the

equation

$$(1a) \quad \mathcal{C} = \{(x, y) \in \mathbb{C}^2 \mid f(x, y) = 0\},$$

$$(1b) \quad f(x, y) = -y^n + x^s + \sum_{j=0}^{n-2} \sum_{i=0}^{s-2} \lambda_{n.s-in-j.s} y^j x^i,$$

$$(1c) \quad \lambda_{k \leq 0} = 0, \quad \lambda_k \in \mathbb{C}.$$

where λ_k serve as parameters of the curve, and k shows the Sato weight of λ_k . Only parameters with positive Sato weights are allowed. The Sato weights of x and y are $\text{wgt } x = n$, and $\text{wgt } y = s$. Then $\text{wgt } f(x, y) = ns$. Note, that some terms are omitted in (1), since the definition contains the minimal number of parameters. All other terms can be eliminated by a proper bi-rational transformation.

Due to n and s are co-prime, infinity is the Weierstrass point where all n sheets of the curve join. Let ξ denote a local parameter near infinity, then

$$(2) \quad x = \xi^{-n}, \quad y = \xi^{-s}(1 + O(\lambda))$$

gives the simplest parametrization of (1). Evidently, the Sato weight equals the opposite to the exponent of the leading term in the expansion near infinity.

2.2. Abel map and theta function. Let $du = (du_{\mathfrak{w}_1}, du_{\mathfrak{w}_2}, \dots, du_{\mathfrak{w}_g})^t$ be not normalized first kind differentials, labeled by elements of the Weierstrass gap sequence $\{\mathfrak{w}_1, \mathfrak{w}_2, \dots, \mathfrak{w}_g\}$, which coincide with negative Sato weights: $\text{wgt } du_{\mathfrak{w}_i} = -\mathfrak{w}_i$, and show the orders of zero at infinity.

Let the Abel map \mathcal{A} be defined with respect to not normalized differentials:

$$(3) \quad \mathcal{A}(P) = \int_{\infty}^P du, \quad P = (x, y) \in \mathcal{C}.$$

Here infinity is used as the base point, which is the standard choice in the case of (n, s) -curves. If a curve is not an (n, s) -one, the base point is chosen among Weierstrass points on the curve.

First kind integrals along canonical homology cycles $\{\mathfrak{a}_i, \mathfrak{b}_i\}_{i=1}^g$ give first kind period matrices:

$$\omega = (\omega_{ij}) = \left(\int_{\mathfrak{a}_j} du_i \right), \quad \omega' = (\omega'_{ij}) = \left(\int_{\mathfrak{b}_j} du_i \right).$$

Columns of ω, ω' generate the lattice \mathfrak{P} of periods. Then $\text{Jac}(\mathcal{C}) = \mathbb{C}^g \setminus \mathfrak{P}$ is the Jacobian variety of the curve \mathcal{C} .

The theta function is defined in terms of normalized coordinates $v = \omega^{-1}u$ and normalized periods $(1_g, \tau)$, where 1_g denotes the identity matrix of size g , and $\tau = \omega^{-1}\omega'$. Matrix τ is symmetric with a positive imaginary part: $\tau^t = \tau$, $\text{Im } \tau > 0$, that is τ belongs to the Siegel upper half-space. The normalised first kind differentials are defined by

$$dv = \omega^{-1}du,$$

and the Abel map $\bar{\mathcal{A}}$ with respect to the normalised differentials is

$$(4) \quad \bar{\mathcal{A}}(P) = \int_{\infty}^P dv, \quad P = (x, y) \in \mathcal{C}.$$

2.3. Theta and sigma functions. Recall the two entire functions on $\mathbb{C}^g \supset \text{Jac}(\mathcal{C})$, which generate multiply periodic (or Abelian) functions, and so serve for uniformization of a curve \mathcal{C} .

The Riemann *theta function*

$$\theta(v; \tau) = \sum_{n \in \mathbb{Z}^g} \exp(i\pi n^t \tau n + 2i\pi n^t v).$$

is defined in terms of normalized coordinates $v = \omega^{-1}u$, $u \in \text{Jac}(\mathcal{C})$, and normalized period matrix τ . A theta function with characteristic is defined by

$$(5) \quad \theta[\varepsilon](v; \tau) = \exp(i\pi(\frac{1}{2}\varepsilon'^t)\tau(\frac{1}{2}\varepsilon') + 2i\pi(v + \frac{1}{2}\varepsilon)^t(\frac{1}{2}\varepsilon'))\theta(v + \frac{1}{2}\varepsilon + \tau(\frac{1}{2}\varepsilon'); \tau),$$

where a characteristic is represented by a $2 \times g$ matrix $[\varepsilon] = (\varepsilon', \varepsilon)^t$ with real values within the interval $[0, 2)$. Every point u within the fundamental domain of $\text{Jac}(\mathcal{C})$ can be represented by its characteristic $[\varepsilon]$, namely

$$u = \omega(\frac{1}{2}\varepsilon) + \omega'(\frac{1}{2}\varepsilon').$$

In the hyperelliptic case, the Abel images of branch points and any combination of branch points are described by characteristics with components 1 or 0, which are called half-integer characteristics. Such a characteristic is odd whenever $\varepsilon^t \varepsilon' = 0 \pmod{2}$, and even whenever $\varepsilon^t \varepsilon' = 1 \pmod{2}$. A theta function with half-integer characteristic has the same parity as its characteristic.

The modular invariant entire function on $\text{Jac}(\mathcal{C})$ is called the *sigma function*. As a definition we use its relation with the theta function:

$$(6) \quad \sigma(u) = C \exp(-\frac{1}{2}u^t \varkappa u) \theta[K](\omega^{-1}u; \omega^{-1}\omega'),$$

where $[K]$ denotes the characteristic of the vector of Riemann constants, and $\varkappa = \eta\omega^{-1}$ is a symmetric matrix. The Sato weight of the sigma function is computed by the formula $\text{wgt } \sigma = -(n^2 - 1)(s^2 - 1)/24$, see [9].

The sigma function is defined in terms of not normalized coordinates u , and not normalized period matrices of the first kind ω , ω' , and of the second kind η , η' . The latter are defined as follows

$$\eta = (\eta_{ij}) = \left(\int_{\mathfrak{a}_j} dr_i \right), \quad \eta' = (\eta'_{ij}) = \left(\int_{\mathfrak{b}_j} dr_i \right)$$

with the help of second kind differentials $dr = (dr_{\mathfrak{w}_1}, dr_{\mathfrak{w}_2}, \dots, dr_{\mathfrak{w}_g})^t$. It is important to choose the second kind differentials which form an associated system with differentials of the first kind, see [2, Art. 138]. Note that $dr_{\mathfrak{w}_i}$ has the only pole of order \mathfrak{w}_i at infinity, and so $\text{wgt } r_{\mathfrak{w}_i} = \mathfrak{w}_i$. In the vicinity of infinity, $\xi(\infty) = 0$, the following relation holds

$$(7) \quad \text{res}_{\xi=0} \left(\int_0^\xi du(\tilde{\xi}) \right) dr(\xi)^t = 1_g,$$

where 1_g is the identity matrix of order g . The relation completely determines the principle part of $dr(\xi)$.

The not normalized periods matrices of the first ω , ω' and second η , η' kinds satisfy the Legendre relation

$$(8) \quad \Omega^t \mathbf{J} \Omega = 2\pi i \mathbf{J},$$

$$\Omega = \begin{pmatrix} \omega & \omega' \\ \eta & \eta' \end{pmatrix}, \quad \mathbf{J} = \begin{pmatrix} 0 & -1_g \\ 1_g & 0 \end{pmatrix}.$$

Multiply periodic \wp -functions are defined with the help of the sigma function:

$$\wp_{i,j}(u) = -\frac{\partial^2 \log \sigma(u)}{\partial u_i \partial u_j}, \quad \wp_{i,j,k}(u) = -\frac{\partial^3 \log \sigma(u)}{\partial u_i \partial u_j \partial u_k}.$$

From (6) we obtain expressions in terms of the theta function:

$$(9) \quad \begin{aligned} \wp_{i,j}(u) &= \varkappa_{i,j} - \frac{\partial^2}{\partial u_i \partial u_j} \log \theta[K](\omega^{-1}u; \omega^{-1}\omega'), \\ \wp_{i,j,k}(u) &= -\frac{\partial^3}{\partial u_i \partial u_j \partial u_k} \log \theta[K](\omega^{-1}u; \omega^{-1}\omega'). \end{aligned}$$

The vector of Riemann constants K with respect to a base point P_0 is defined by the formula, [16, Eq. (2.4.14)]

$$(10) \quad K_j = \frac{1}{2}(1 + \tau_{j,j}) - \sum_{l \neq j} \oint_{a_l} dv_j(P) \int_{P_0}^P dv_l, \quad j = 1, \dots, g.$$

In the hyperelliptic case, the vector is computed¹ in [18, p. 14], and equals the sum of all odd characteristics of the fundamental set of $2g + 1$ characteristics which represent branch points, according to [2, Art.200–202].

2.4. Bolza formulas and generalizations. In genus 2, expressions for branch points in terms of the theta function are known as the Bolza formulas

$$e_\iota = -\frac{\partial_{u_3} \theta[\{\iota\}](\omega^{-1}u)}{\partial_{u_1} \theta[\{\iota\}](\omega^{-1}u)} \Big|_{u=0},$$

where $[\{\iota\}]$ denotes the characteristic corresponding to the branch point e_ι , see [8, Eq. (6)]. A generalization of the Bolza formulas for a hyperelliptic curve of arbitrary genus g is obtained in [12]. In particular,

$$e_\iota = -\frac{\partial_{u_{2(g \bmod 2)+1, \dots, u_{2g-7}, u_{2g-1}}}^{[g/2]} \theta[\{\iota\}](\omega^{-1}u)}{\partial_{u_{2(g \bmod 2)+1, \dots, u_{2g-7}, u_{2g-3}}}^{[g/2]} \theta[\{\iota\}](\omega^{-1}u)} \Big|_{u=0}.$$

2.5. Jacobi inversion problem. Given a point u of the Jacobian variety $\text{Jac}(\mathcal{C})$ find a reduced divisor $D \in \mathcal{C}^g$ such that $\mathcal{A}(D) = u$. Every class of linearly equivalent divisors on a curve of genus g has a representative of degree g or less, which is called a reduced divisor. Reduced divisors of degree less than g are special, and the Riemann theta function vanishes on such divisors, according to the Riemann vanishing theorem. Reduced divisors of degree g are called non-special. Every non-special divisor represents its class uniquely.

A solution of the Jacobi inversion problem is known for non-special divisors. On hyperelliptic curves such a solution was given in [2, Art. 216] and rediscovered in [10, Theorem 2.2]. Let a non-degenerate hyperelliptic curve of genus g be defined² by

$$(11) \quad -y^2 + x^{2g+1} + \sum_{i=1}^{2g} \lambda_{2i+2} x^{2g-i} = 0.$$

¹We use a homology basis different from [18], and so $[K]$ is not exactly the same, but computed in a similar way.

²A $(2, 2g + 1)$ -curve serves as a canonical form of hyperelliptic curves of genus g .

Let $u = \mathcal{A}(D)$ be the Abel image of a degree g non-special divisor D on the curve. Then D is uniquely defined by the system of equations

$$(12a) \quad \mathcal{R}_{2g}(x; u) \equiv x^g - \sum_{i=1}^g x^{g-i} \wp_{1,2i-1}(u) = 0,$$

$$(12b) \quad \mathcal{R}_{2g+1}(x, y; u) \equiv 2y + \sum_{i=1}^g x^{g-i} \wp_{1,1,2i-1}(u) = 0.$$

On a trigonal curve, the Jacobi inversion problem is solved in [11]. A method of obtaining such a solution on a curve of an arbitrary gonality is presented in [7]; trigonal, tetragonal and pentagonal curves are considered as an illustration. In the case of a $(3, 3m+1)$ -curve, a degree g non-special divisor D such that $u = \mathcal{A}(D)$ is given by the system

$$(13a) \quad \mathcal{R}_{6m+1}(x, y; u) \equiv x^{2m} - y \sum_{i=1}^m \wp_{1,3i-2}(u) x^{m-i} - \sum_{i=1}^{2m} \wp_{1,3i-1}(u) x^{2m-i} = 0,$$

$$(13b) \quad \mathcal{R}_{6m+2}(x, y; u) \equiv 2yx^m + y \sum_{i=1}^m (\wp_{1,1,3i-2}(u) - \wp_{2,3i-2}(u)) x^{m-i} \\ + \sum_{i=1}^{2m} (\wp_{1,1,3i-1}(u) - \wp_{2,3i-1}(u)) x^{2m-i} = 0.$$

In the case of a $(3, 3m+2)$ -curve, by the system

$$(14a) \quad \mathcal{R}_{6m+2}(x, y; u) \equiv yx^m - y \sum_{i=1}^m \wp_{1,3i-1}(u) x^{m-i} \\ - \sum_{i=1}^{2m+1} \wp_{1,3i-2}(u) x^{2m+1-i} = 0,$$

$$(14b) \quad \mathcal{R}_{6m+3}(x, y; u) \equiv 2x^{2m+1} + y \sum_{i=1}^m (\wp_{1,1,3i-1}(u) - \wp_{2,3i-1}(u)) x^{m-i} \\ - \sum_{i=1}^{2m+1} (\wp_{1,1,3i-2}(u) - \wp_{2,3i-2}(u)) x^{2m+1-i} = 0.$$

3. PERIODS ON A HYPERELLIPTIC CURVE

Hyperelliptic are the best known plane algebraic curves. There exists a universal approach to homology and cohomology basis, as well as constructing a Riemann surface. Therefore, this type of curves is considered separately.

3.1. Hyperelliptic curves. Let a generic hyperelliptic curve be defined by

$$(15) \quad 0 = f(x, y) = -y^2 + y\mathcal{Q}(x) + \mathcal{P}(x),$$

where $\deg \mathcal{P} = 2g+1$ or $2g+2$, in the case of genus g .

An equation with $\deg \mathcal{P} = 2g+1$, $\mathcal{Q}(x) \equiv 0$ defines an (n, s) -curve, which is considered as the canonical form of a hyperelliptic curve of genus g :

$$0 = f(x, y) = -y^2 + x^{2g+1} + \lambda_4 x^{2g-1} + \dots + \lambda_{4g} x + \lambda_{4g+2}.$$

Sato weights are $\text{wgt } x = 2$, $\text{wgt } y = 2g + 1$, and so $\text{wgt } f = 4g + 2$. The term $\lambda_2 x^{2g}$ of a generic \mathcal{P} is eliminated by a proper Möbius transformation, and $y\mathcal{Q}(x)$ is eliminated by the map $y \mapsto \tilde{y} + \frac{1}{2}\mathcal{Q}(x)$, which leads to

$$0 = f(x, y) = -\tilde{y}^2 + \tilde{\mathcal{P}}(x), \quad \tilde{\mathcal{P}}(x) = \mathcal{P}(x) + \frac{1}{4}\mathcal{Q}(x)^2.$$

Thus, the discriminant of (15) is defined by the formula

$$(16) \quad \Delta(x) = \tilde{\mathcal{P}}(x) = \mathcal{P}(x) + \frac{1}{4}\mathcal{Q}(x)^2.$$

A canonical curve can be defined by its branch points $\{(e_i, 0)\}_{i=1}^{2g+1}$, namely

$$(17) \quad 0 = f(x, y) = -y^2 + \mathcal{P}(x), \quad \mathcal{P}(x) = \prod_{j=1}^{2g+1} (x - e_j).$$

For the sake of brevity, the notation e_i is employed both for a branch point $(e_i, 0)$ and its x -coordinate, in the hyperelliptic case. If all branch points are distinct, then the curve is non-degenerate, and its genus equals g . The curve (17) has also a branch point located at infinity ∞ , referred also as e_0 . If $\sum_{i=1}^{2g+1} e_i = 0$, then $\lambda_2 = 0$. However, we omit the latter condition, and allow $\{e_i\}$ be arbitrary.

A curve with $\deg \mathcal{P} = 2g + 2$, and $\mathcal{Q}(x) \equiv 0$ has $2g + 2$ finite branch points, denoted by $\{(e_i, 0)\}_{i=0}^{2g+1}$. The corresponding canonical form is obtained by moving the finite branch point e_0 to infinity.

In the generic case (15), the maximal $\deg \mathcal{Q}$ equals g , due to respect to the Sato weight. Such a curve can be defined by choosing arbitrary values $\{e_i\}$ of number $2g + 1$ or $2g + 2$, and choosing a polynomial \mathcal{Q} of degree up to g . Then the corresponding y -coordinates of branch points $\{(e_i, h_i)\}$ are obtained by the formula $h_i = \frac{1}{2}\mathcal{Q}(e_i)$.

The gap sequence on a hyperelliptic curve (15) is

$$\mathfrak{W} = \{\mathfrak{w}_i = 2i - 1 \mid i = 1, \dots, g\}.$$

In what follows, we focus on the canonical form of a hyperelliptic curve.

3.2. Homology. Let $\{e_i\}_{i=1}^{2g+1}$ be complex numbers, sorted ascendingly first by the real part, then the imaginary part.

Cuts are made between points e_{2k-1} and e_{2k} with k from 1 to g , and from e_{2g+1} to infinity ∞ . With k running from 1 to g an \mathfrak{a}_k -cycle encircles the cut (e_{2k-1}, e_{2k}) counter-clockwise, and a \mathfrak{b}_k -cycle enters into the cut (e_{2k-1}, e_{2k}) and comes out from the cut (e_{2g+1}, ∞) , see fig. 1 as an example. This canonical homology basis is adopted from Baker [2, p. 303].

Remark 1. In the case of $\deg \mathcal{P} = 2g + 2$, with branch points $\{(e_i, 0)\}_{i=0}^{2g+1}$, we sort the latter in the same way as in the canonical case. So e_0 has the smallest real and imaginary part among all branch points. Cuts are made between points e_{2k-1} and e_{2k} with k from 1 to g , and from e_{2g+1} to e_0 through infinity. A canonical homology basis is introduced in a similar way: an \mathfrak{a}_k -cycle encircles the cut (e_{2k-1}, e_{2k}) counter-clockwise, and a \mathfrak{b}_k -cycle enters into the cut (e_{2k-1}, e_{2k}) and comes out from the cut $e_{2g+1}-\infty-e_0$.

3.3. Cohomology. First kind differentials are defined in the standard way, see [2, p. 306] for example,

$$(18) \quad du_{2i-1} = \frac{x^{g-i} dx}{\partial_y f(x, y)}, \quad i = 1, \dots, g.$$

On the canonical hyperelliptic curve, the second kind differentials associated with the first kind ones have the form

$$(19) \quad dr_{2i-1} = \frac{dx}{\partial_y f(x, y)} \sum_{k=1}^{2i-1} k \lambda_{4i-2k+2} x^{g-i+k}, \quad i = 1, \dots, g.$$

3.4. Riemann surface. At every point x , except branch points, there exist two values of y ($s = \pm 1$):

$$(20a) \quad y_s(x) = s\sqrt{\Delta(x)}, \quad \Delta(x) = \mathcal{P}(x), \quad \text{in the canonical case,} \quad \text{or}$$

$$(20b) \quad y_s(x) = \frac{1}{2}\mathcal{Q}(x) + s\sqrt{\Delta(x)}, \quad \text{in the generic case.}$$

The *key element* of the proposed scheme of analytic computation is how to draw a continuous path on each sheet of the Riemann surface of a curve. To answer this question, we define the square root function as follows

$$(21) \quad \sqrt{\Delta(x)} = \begin{cases} \sqrt{|\Delta(x)|} e^{(\iota/2) \arg \Delta(x)} & \text{if } \arg \Delta(x) \geq 0, \\ \sqrt{|\Delta(x)|} e^{(\iota/2) \arg \Delta(x) + \iota\pi} & \text{if } \arg \Delta(x) < 0, \end{cases}$$

where \arg has the range $(-\pi, \pi]$. With such a definition the range of $\arg \sqrt{\Delta(x)}$ is $[0, \pi)$. Moreover,

Theorem 1. *Let $\sqrt{\Delta}$ be defined by (21). Then y defined by (20) has a discontinuity over the contour $\Gamma = \{x \mid \arg \Delta(x) = 0\}$, and y_+ serves as the analytic continuation of y_- , and vice versa on the other side of the contour.*

Proof. Let \tilde{x} be located in the vicinity of the contour Γ , more precisely $|\arg \Delta(\tilde{x})| < 2\phi$, with a small positive value ϕ . Then $0 \leq \arg \sqrt{\Delta(\tilde{x})} < \phi$ if $\arg \Delta(\tilde{x}) \geq 0$, and $\pi - \phi < \arg \sqrt{\Delta(\tilde{x})} < \pi$ if $\arg \Delta(\tilde{x}) < 0$. Evidently, the discontinuity of $\sqrt{\Delta}$ is located on the contour Γ .

Next, we find the analytic continuation of $\sqrt{\Delta}$. Let $U(x_0; \delta)$ be a disc of radius δ with the center at $x_0 \in \Gamma$. The contour Γ divides the disc into two parts: U_+ where $\arg \Delta(x) \geq 0$, and U_- where $\arg \Delta(x) < 0$. The analytic continuation of $\sqrt{\Delta}$ from U_+ to U_- is given by $-\sqrt{\Delta}$, since the range of $\arg(-\sqrt{\Delta(x)}) = \arg(e^{-\iota\pi} \sqrt{\Delta(x)})$ is $[-\pi, 0)$. On the other hand, the analytic continuation of $\sqrt{\Delta}$ from U_- to U_+ is given by $-\sqrt{\Delta} = e^{\iota\pi} \sqrt{\Delta}$. \square

With the help of definition (21), we fix the position of discontinuity of $\sqrt{\Delta}$ at the contour Γ where $\arg \Delta(x) = 0$. So the knowledge about location of the contour Γ on the complex plane of x solves the problem how to draw a continuous path. Actually, at any intersection with Γ the sign s in (20) changes into the opposite. This rule guaranties that the path remains on the same sheet.

Let a continuous path starts at infinity as $x \rightarrow -\infty$, goes through all branch points in the chosen order, and ends at infinity as $x \rightarrow \infty$, see fig. 2 for example.

3.5. Computation of periods. An algorithm of obtaining first kind periods on a canonical hyperelliptic curve is given below.

1. Let all branch points $\{e_i\}_{i=1}^{2g+1}$ be sorted in the ascending order of real and imaginary parts. Connect pairs of points by straight line segments $[e_i, e_{i+1}]$, $i = 1, \dots, 2g$. Join the segment $(-\infty, e_1]$ at the beginning of the polygonal path, and $[e_{2g+1}, \infty)$ at the end. This is the required path through all branch points, marked in orange on fig. 2.
2. Plot the contour $\Gamma = \{x \mid \arg \mathcal{P}(x) = 0\}$, see blue contours on fig. 2. Find the sequence of signs $\{\mathfrak{s}_{0,1}\} \cup \{\mathfrak{s}_{i,i+1}\}_{i=1}^{2g} \cup \{\mathfrak{s}_{2g+1,0}\}$ on all segments of the polygonal path, taking into account intersections with Γ . Index 0 is used for infinity. Every cut is rounded in the counter-clockwise direction. On fig. 2, a curved orange line near a cut shows which side of the cut is chosen.
3. Compute first kind integrals on each segment along the polygonal path

$$(22a) \quad \mathcal{A}_{i,i+1} = \int_{e_i}^{e_{i+1}} du, \quad i = 1, \dots, 2g,$$

$$(22b) \quad \mathcal{A}_{0,1} = \int_{-\infty}^{e_1} du, \quad \mathcal{A}_{2g+1,0} = \int_{e_{2g+1}}^{\infty} du.$$

The integrand of $\mathcal{A}_{i,j}$ is taken with the sign $\mathfrak{s}_{i,j}$, that is

$$du = \begin{pmatrix} x^{g-1} \\ \vdots \\ x \\ 1 \end{pmatrix} \frac{dx}{-2\mathfrak{s}_{i,j}\sqrt{\mathcal{P}(x)}}.$$

Due to the involution of a hyperelliptic curve, the following relations hold

$$(23a) \quad \sum_{i=1}^g \mathcal{A}_{2i-1,2i} + \mathcal{A}_{2g+1,0} = 0,$$

$$(23b) \quad \mathcal{A}_{0,1} + \sum_{i=1}^g \mathcal{A}_{2i,2i+1} = 0.$$

The latter are used for verification.

4. According to the choice of canonical cycles, columns of the first kind period matrices are

$$(24) \quad \omega_k = 2\mathcal{A}_{2k-1,2k}, \quad \omega'_k = -2 \sum_{j=k}^g \mathcal{A}_{2j,2j+1}.$$

The normalized period matrix is obtain by

$$\tau = \omega^{-1}\omega',$$

and required to be symmetric with positive imaginary part.

This analytic approach is used in numerical computation of periods with the help of Wolfram Mathematica 12. The function `NIntegrate` is used to compute (22).

3.6. Example 1: Arbitrary complex branch points. Let a hyperelliptic curve of genus 4 possesses the given finite branch points:

$$-18 - 2i, -16 + 5i, -11 + 3i, -10 - i, -4 + 2i, -3 + 3i, 3 + 3i, 7 - 2i, 13 - i,$$

and a branch point at infinity.

On the other hand, this curve is defined by the equation

$$(25a) \quad 0 = f(x, y) = -y^2 + \mathcal{P}(x),$$

$$(25b) \quad \begin{aligned} \mathcal{P}(x) = & x^9 + (39 - 10i)x^8 + (217 - 288i)x^7 - (7585 - 826i)x^6 \\ & - (79138 - 82462i)x^5 + (324058 + 455846i)x^4 + (4126332 - 3930980i)x^3 \\ & - (14219032 + 29444932i)x^2 - (131012592 - 28208616i)x \\ & - 101860560 + 245519280i. \end{aligned}$$

Cuts and homology cycles, see fig.1, are introduced as explained in subsections 3.2 and 3.3. On fig.2, the contour Γ is shown in blue, and a continuous path in

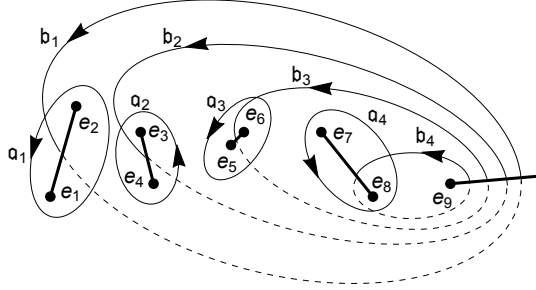


FIGURE 1. Canonical homology cycles.

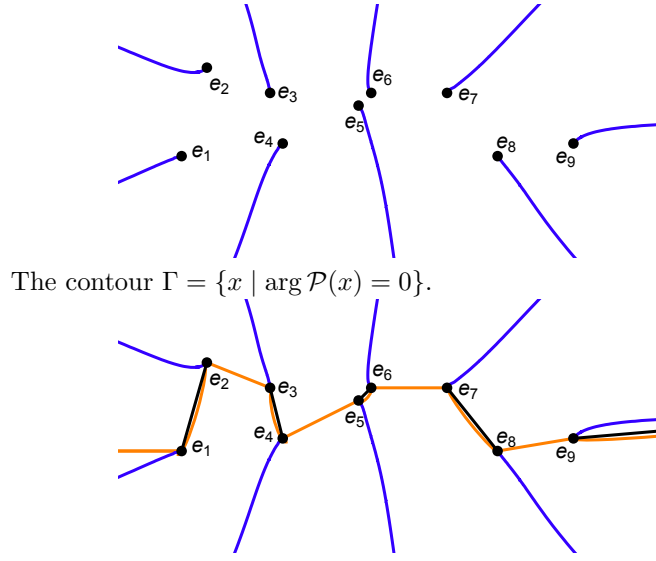
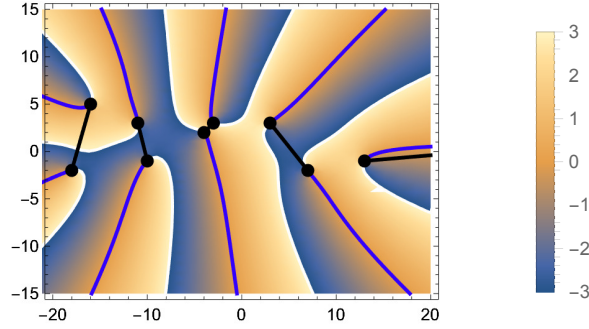
orange. Fig. 3 shows the density plot of $\arg \mathcal{P}(x)$ over the domain $-20 \leq \operatorname{Re} x \leq 20$, $-15 \leq \operatorname{Im} x \leq 15$.

Let start with $s_{0,1} = +1$ on segment $(-\infty, e_1]$. The orange path intersects the blue contour at point e_1 , and so the sign changes: $s_{1,2} = -1$. The path goes along the right side of the cut (e_1, e_2) , and the sign remains the same on the next segment: $s_{2,3} = -1$. From e_3 to e_4 the path goes along the left side of the cut (e_3, e_4) , so the sign remains the same: $s_{3,4} = -1$. The next intersection with the blue contour occurs at point e_4 , thus $s_{4,5} = +1$. And again at point e_5 , so $s_{5,6} = s_{6,7} = s_{7,8} = -1$. Once again, the path intersects the blue contour at point e_8 , thus $s_{8,9} = s_{9,0} = +1$. Finally, the sequence of signs is

$$\begin{aligned} & \{s_{0,1}, s_{1,2}, s_{2,3}, s_{3,4}, s_{4,5}, s_{5,6}, s_{6,7}, s_{7,8}, s_{8,9}, s_{9,0}\} = \\ \text{Sheet 1: } & \{+1, -1, -1, -1, +1, -1, -1, -1, +1, +1\}. \end{aligned}$$

First kind differentials as functions of x are

$$du \equiv \begin{pmatrix} du_1 \\ du_3 \\ du_5 \\ du_7 \end{pmatrix} = \begin{pmatrix} x^3 \\ x^2 \\ x \\ 1 \end{pmatrix} \frac{dx}{-2s\sqrt{\mathcal{P}(x)}}.$$

FIGURE 2. A continuous path (orange), and the contour Γ (blue).FIGURE 3. Density plot of $\arg \mathcal{P}(x)$, and the contour Γ (in blue).

According to the picture of homology cycles, see fig.1, the first kind period matrices ω and ω' are

$$\omega = 2(\mathcal{A}_{1,2}, \mathcal{A}_{3,4}, \mathcal{A}_{5,6}, \mathcal{A}_{7,8}),$$

$$\omega' = -2(\mathcal{A}_{2,3} + \mathcal{A}_{4,5} + \mathcal{A}_{6,7} + \mathcal{A}_{8,9}, \mathcal{A}_{4,5} + \mathcal{A}_{6,7} + \mathcal{A}_{8,9}, \mathcal{A}_{6,7} + \mathcal{A}_{8,9}, \mathcal{A}_{8,9}).$$

On the curve (25) we have

$$\omega \approx \begin{pmatrix} -1.303573 + 0.207439i & 0.848115 - 0.306788i \\ 0.073367 - 0.003075i & -0.083799 + 0.019801i \\ -0.003985 - 0.000333i & 0.008037 - 0.001042i \\ 0.000208 + 0.000046i & -0.000751 + 0.000028i \\ 0.0166625 + 0.063503i & -0.035439 - 0.017840i \\ 0.005372 - 0.014707i & -0.007363 - 0.005200i \\ -0.003023 + 0.002108i & -0.001651 - 0.000958i \\ 0.000856 + 0.000006i & -0.000350 - 0.000098i \end{pmatrix},$$

$$\omega' \approx \begin{pmatrix} -0.604960 - 0.930374i & -0.085127 + 0.237963i \\ 0.029948 + 0.024444i & 0.019758 - 0.067832i \\ -0.001525 - 0.000835i & -0.002854 + 0.005901i \\ 0.000078 + 0.000029i & 0.000324 - 0.000426i \\ & 0.042341 - 0.110642i & 0.047121 - 0.129831i \\ & 0.011312 - 0.018512i & 0.006638 - 0.011849i \\ & -0.002257 - 0.001647i & 0.000894 - 0.001058i \\ & 0.000178 + 0.000796i & 0.000117 - 0.000089i \end{pmatrix}.$$

The corresponding normalized period matrix from the Siegel upper half-space is

$$\tau \approx \begin{pmatrix} 0.416960 + 1.348235i & -0.019631 + 0.866637i \\ -0.019631 + 0.866637i & -0.401986 + 1.468494i \\ 0.043442 + 0.592788i & 0.090347 + 0.771653i \\ 0.013536 + 0.360353i & 0.020075 + 0.430424i \\ & 0.043442 + 0.592788i & 0.013536 + 0.360353i \\ & 0.090347 + 0.771653i & 0.020075 + 0.430424i \\ & 0.276110 + 1.677311i & -0.019449 + 0.549477i \\ & -0.019449 + 0.549477i & -0.241045 + 0.959518i \end{pmatrix}.$$

Using the second kind differentials

$$(26) \quad dr_{2i-1} = \frac{\mathcal{R}_{2i-1}(x) dx}{-2s\sqrt{\mathcal{P}(x)}}, \quad i = 1, 2, 3, 4,$$

$$\begin{aligned} \mathcal{R}_1 &= x^4, \\ \mathcal{R}_3 &= 3x^5 + (78 - 20i)x^4 + (217 - 288i)x^3, \\ \mathcal{R}_5 &= 5x^6 + (156 - 40i)x^5 + (651 - 864i)x^4 - (15170 - 1652i)x^3 \\ &\quad - (79138 - 82462i)x^2, \\ \mathcal{R}_7 &= 7x^7 + (234 - 60i)x^6 + (1085 - 1440i)x^5 - (30340 - 3304i)x^4 \\ &\quad - (237414 - 247386i)x^3 + (648116 + 911692i)x^2 \\ &\quad + (4126332 - 3930980i)x. \end{aligned}$$

we compute second kind periods

$$\eta \approx \begin{pmatrix} 22.428062 - 6.098673i & -8.281570 + 4.260894i \\ 280.811215 - 73.921437i & -233.173130 + 22.293105i \\ 910.855655 + 10.721526i & -2603.233939 - 813.570166i \\ 1224.707652 + 409.922637i & -7484.857429 - 1328.792554i \\ & -0.205360 - 0.177582i & -0.198185 - 0.006055i \\ & 5.630286 - 0.370818i & -32.028810 + 11.479858i \\ & 299.647570 + 719.376216i & 1242.433044 + 350.238889i \\ & 487.787097 + 8861.332415i & 6189.443173 - 7889.884228i \end{pmatrix},$$

$$\eta' \approx \begin{pmatrix} 13.855811 + 9.185567i & 1.880170 - 4.181065i \\ 150.913701 + 40.841618i & 64.433701 - 272.113911i \\ 420.612695 + 72.624802i & 1188.248232 - 1359.820959i \\ 504.296929 + 98.209496i & 3559.979547 - 2711.948811i \end{pmatrix}$$

$$\begin{pmatrix} 0.264151 - 1.540944\iota & 0.305811 - 1.421979\iota \\ -26.525723 - 208.762530\iota & -27.152420 - 206.017\iota \\ -1290.627353 - 496.867943\iota & -1470.266735 - 1061.435845\iota \\ -9584.859568 + 9412.897457\iota & -2002.776466 + 2196.979511\iota \end{pmatrix}.$$

and the symmetric matrix

$$\varkappa \approx \begin{pmatrix} -26.150273 + 5.226639\iota & -113.639362 + 91.745099\iota \\ -113.639362 + 91.745099\iota & 2527.918193 + 333.2000001\iota \\ 815.048336 + 59.142845\iota & 6691.213749 - 15142.962600\iota \\ 2796.548807 - 2715.208601\iota & -19805.451622 - 22245.716646\iota \\ 815.048336 + 59.142845\iota & 2796.548807 - 2715.208601\iota \\ 6691.213749 - 15142.962600\iota & -19805.451622 - 22245.716646\iota \\ -501204.576087 - 151451.871496\iota & -1572965.591976 + 1699015.043174\iota \\ -1572965.591976 + 1699015.043174\iota & -403196.119224 + 19865411.502694\iota \end{pmatrix}.$$

Numerical integration is performed with the working precision of 18. The same accuracy is achieved in the relations (23), and at most 16-digit precision in verification of the symmetric property of τ . The symmetric property of \varkappa is satisfied with the accuracy of 10^{-8} . The Legendre relations are accurate up to 10^{-14} .

Verification. An analog of the Bolza formulas on a genus 4 hyperelliptic curve, see [5, Eq. (40)], is given by

$$(27) \quad e_\iota = -\frac{\partial_{u_1, u_7}^2 \theta[\{\iota\}](\omega^{-1}u)}{\partial_{u_1, u_5}^2 \theta[\{\iota\}](\omega^{-1}u)} \Big|_{u=0}.$$

According to the construction of the basis, we have the following correspondence between characteristics and branch points:

$$\begin{aligned} e_1 = -18 - 2\iota & \quad [\varepsilon_1] = \begin{pmatrix} 1 & 0 & 0 & 0 \\ 0 & 0 & 0 & 0 \end{pmatrix} & \quad [\{1\}] = \begin{pmatrix} 0 & 1 & 1 & 1 \\ 0 & 1 & 0 & 1 \end{pmatrix}, \\ e_2 = -16 + 5\iota & \quad [\varepsilon_2] = \begin{pmatrix} 1 & 0 & 0 & 0 \\ 1 & 0 & 0 & 0 \end{pmatrix} & \quad [\{2\}] = \begin{pmatrix} 0 & 1 & 1 & 1 \\ 1 & 1 & 0 & 1 \end{pmatrix}, \\ e_3 = -11 + 3\iota & \quad [\varepsilon_3] = \begin{pmatrix} 0 & 1 & 0 & 0 \\ 1 & 0 & 0 & 0 \end{pmatrix} & \quad [\{3\}] = \begin{pmatrix} 1 & 0 & 1 & 1 \\ 1 & 1 & 0 & 1 \end{pmatrix}, \\ e_4 = -10 - \iota & \quad [\varepsilon_4] = \begin{pmatrix} 0 & 1 & 0 & 0 \\ 1 & 1 & 0 & 0 \end{pmatrix} & \quad [\{4\}] = \begin{pmatrix} 1 & 0 & 1 & 1 \\ 1 & 0 & 0 & 1 \end{pmatrix}, \\ e_5 = -4 + 2\iota & \quad [\varepsilon_5] = \begin{pmatrix} 0 & 0 & 1 & 0 \\ 1 & 1 & 0 & 0 \end{pmatrix} & \quad [\{5\}] = \begin{pmatrix} 1 & 1 & 0 & 1 \\ 1 & 0 & 0 & 1 \end{pmatrix}, \\ e_6 = -3 + 3\iota & \quad [\varepsilon_6] = \begin{pmatrix} 0 & 0 & 1 & 0 \\ 1 & 1 & 1 & 0 \end{pmatrix} & \quad [\{6\}] = \begin{pmatrix} 1 & 1 & 0 & 1 \\ 1 & 0 & 1 & 1 \end{pmatrix}, \\ e_7 = 3 + 3\iota & \quad [\varepsilon_7] = \begin{pmatrix} 0 & 0 & 0 & 1 \\ 1 & 1 & 1 & 0 \end{pmatrix} & \quad [\{7\}] = \begin{pmatrix} 1 & 1 & 1 & 0 \\ 1 & 0 & 1 & 1 \end{pmatrix}, \\ e_8 = 7 - 2\iota & \quad [\varepsilon_8] = \begin{pmatrix} 0 & 0 & 0 & 1 \\ 1 & 1 & 1 & 1 \end{pmatrix} & \quad [\{8\}] = \begin{pmatrix} 1 & 1 & 1 & 0 \\ 1 & 0 & 1 & 0 \end{pmatrix}, \\ e_9 = 13 - \iota & \quad [\varepsilon_9] = \begin{pmatrix} 0 & 0 & 0 & 0 \\ 1 & 1 & 1 & 1 \end{pmatrix} & \quad [\{9\}] = \begin{pmatrix} 1 & 1 & 1 & 1 \\ 1 & 0 & 1 & 0 \end{pmatrix}, \end{aligned}$$

where $[\iota] = [\varepsilon_\iota] + [K]$, and

$$(28) \quad [K] = \sum_{i=1}^4 [\varepsilon_{2i}] = \begin{pmatrix} 1 & 1 & 1 & 1 \\ 0 & 1 & 0 & 1 \end{pmatrix}.$$

The zero matrix serves as the characteristic $[\varepsilon_0]$ of the branch point at infinity e_0 . The method of computing characteristics is adopted from [17].

The formulas (27) are satisfied with the accuracy 10^{-14} .

Remark 2. Period matrices of the first kind obtained for the curve (25) with the help of `algcurses` differ from the presented results, as well as a different and much more entangled homology basis is chosen for computations. The period matrices obtained from `algcurses` satisfy the Bolza formulas for nine half-integer characteristics. The correspondence between characteristics and branch points is not clear from the homology basis, chosen for computation. Although, by computing the Bolza formulas for all characteristics one can find out this correspondence.

3.7. Example 2: Real branch points. Consider briefly the case of a curve (17) with all real branch points:

$$-18, -15, -11, -5, 1, 2, 7, 12, 16,$$

which is defined by the equation

$$(29) \quad 0 = -y^2 + x^9 + 11x^8 - 514x^7 - 4602x^6 + 82441x^5 + 506395x^4 \\ - 4495768x^3 - 11079084x^2 + 54907920x - 39916800.$$

The contour Γ is shown on fig. 4 in blue. In this case, the sequence of signs has

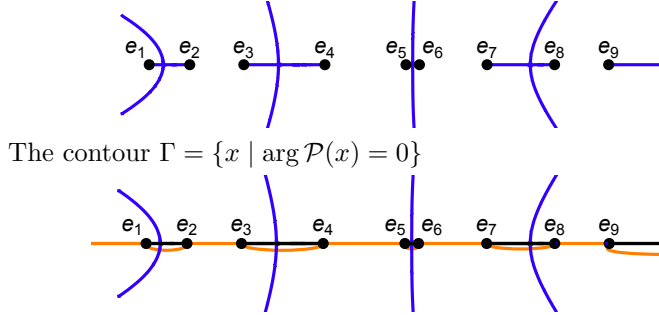


FIGURE 4. A continuous path (orange), and the contour Γ (blue).

a clear pattern:

$$\{s_{0,1}, s_{1,2}, s_{2,3}, s_{3,4}, s_{4,5}, s_{5,6}, s_{6,7}, s_{7,8}, s_{8,9}, s_{9,0}\} = \\ \{+1, -1, -1, +1, +1, -1, -1, +1, +1, -1\}.$$

Note that the cuts are made along horizontal segments of the contour Γ . So, when the path reaches e_1 , the sign changes: $s_{1,2} = -1$. The next change of the sign occurs at e_3 , that is $s_{3,4} = +1$. So, the sign changes at every e_{2i-1} , $i = 1, \dots, g+1$.

With respect to the first kind differentials defined in the previous example, we compute not normalized periods:

$$\omega \approx \begin{pmatrix} -0.675637 & 0.287434 & 0.002651 & -0.309937 \\ 0.041299 & -0.032471 & 0.001599 & -0.031911 \\ -0.002535 & 0.003908 & 0.001010 & -0.003404 \\ 0.000156 & -0.000507 & 0.000673 & -0.000377 \end{pmatrix},$$

$$\omega' \approx \begin{pmatrix} -0.939638i & -0.289356i & -0.312311i & -0.394964i \\ 0.030634i & -0.018895i & -0.013110i & -0.028577i \\ -0.001371i & 0.002447i & 0.001224i & -0.002089i \\ 0.000066i & -0.000232i & 0.000698i & -0.000154i \end{pmatrix}.$$

Then the normalized period matrix from the Siegel upper half-space is

$$\tau \approx \begin{pmatrix} 1.602330i & 0.820786i & 0.514534i & 0.304355i \\ 0.820786i & 1.304404i & 0.648249i & 0.359593i \\ 0.514534i & 0.648249i & 1.686169i & 0.501628i \\ 0.304355i & 0.359593i & 0.501628i & 0.948644i \end{pmatrix}.$$

Remark 3. When all branch points are real, the path through all branch points coincides with the real axis. Moreover, $\mathcal{P}(x)$ is real-valued along the path, positive on segments $[e_{2k-1}, e_{2k}]$, $k = 1, \dots, g+1$, where cuts are made, and negative on the remaining segments $[e_{2k}, e_{2k+1}]$, $k = 0, \dots, g$. If one branch point is located at infinity, then e_0 stands for $-\infty$, end e_{2g+2} stands for ∞ . If all branch points are finite, then e_{2g+2} denotes the same point as e_0 , which is the smallest one.

Since $\mathcal{P}(x)$ has an alternating sign along the path, all \mathbf{a} -periods are real, and all \mathbf{b} -periods are purely imaginary. Moreover,

$$(30) \quad y(x) = (-i)^j \sqrt{|\mathcal{P}(x)|} \quad \text{on a segment } [e_j, e_{j+1}], \quad j = 0, \dots, 2g+1.$$

The formula (30) was discovered by V. Enolsky. It shows how the two analytical solutions connect on one sheet of the Reimann surface.

Second kind periods on (29) computed by (26) with

$$\begin{aligned} \mathcal{R}_1 &= x^4, \\ \mathcal{R}_3 &= 3x^5 + 22x^4 - 514x^3, \\ \mathcal{R}_5 &= 5x^6 + 44x^5 - 1542x^4 - 9204x^3 + 82441x^2, \\ \mathcal{R}_7 &= 7x^7 + 66x^6 - 2570x^5 - 18408x^4 \\ &\quad + 247323x^3 + 1012790x^2 - 4495768x. \end{aligned}$$

are

$$\eta \approx \begin{pmatrix} 11.099150 & -2.673068 & 0.004562 & -3.109806 \\ 42.176466 & -129.207930 & -1.238236 & -5.426458 \\ -383.268207 & -1342.343715 & 100.817590 & 1906.755187 \\ -578.759149 & 4760.249993 & -2368.318297 & -1963.133866 \end{pmatrix},$$

$$\eta' \approx \begin{pmatrix} 3.501174i & -5.136174i & -5.034880i & -5.515607i \\ -11.2650450i & -187.532997i & -174.869192i & -151.780483i \\ -195.044640i & 288.885494i & 811.312906i & 816.306629i \\ -195.450172i & 1246.674997i & 6300.606235i & -562.511001i \end{pmatrix},$$

and the symmetric matrix

$$\varkappa \approx \begin{pmatrix} -13.123159 & 129.285113 & 1107.820797 & -1910.386399 \\ 129.285113 & 1362.173530 & -26772.601447 & 34575.690532 \\ 1107.820797 & -26772.601447 & -519356.757226 & 988034.553637 \\ -1910.386399 & 34575.690532 & 988034.553637 & -5074619.889795 \end{pmatrix}.$$

Numerical integration is performed with the working precision of 18. The same accuracy is achieved in the relations (23), and at most 16-digit precision in verification of the symmetric property of τ . The symmetric property of \varkappa is satisfied

with the accuracy of 10^{-8} . The Legendre relations are accurate up to 10^{-14} . The Legendre relations are accurate up to 10^{-14} .

4. COMPUTATION OF \wp -FUNCTIONS ON A HYPERELLIPTIC CURVE

Given a divisor $D = \sum_{i=1}^n (x_i, y_i)$ on a curve, we compute

$$\mathcal{A}(D) = \sum_{i=1}^n \mathcal{A}(x_i, y_i),$$

using the Abel map (3) with the standard differentials, defined by (18) on a hyperelliptic curve. Then \wp -functions are calculated by means of (9) with $u = \mathcal{A}(D)$. The characteristic of the vector of Riemann constants is computed as a sum of odd characteristics corresponding to branch points, cf. (28). The theta function with this characteristic has the maximal order of vanishing at $v = 0$, which corresponds to the Sato weight of the sigma function, which is $\text{wgt } \sigma = -\frac{1}{2}(g+1)g$.

4.1. Example 1a. We continue to work with the curve (25) from Example 1 in the previous section.

Let u be the Abel map of a non-special divisor $D = \sum_{i=1}^4 (x_i, y_i)$, say

$$\begin{aligned} (x_1, y_1) &= (-9 + \iota, -8\sqrt{-918645 - 541515\iota}) \\ &\approx (-9 + \iota, -2174.219935 + 7969.975679\iota), \\ (x_2, y_2) &= (-3 - 3\iota, -12\sqrt{4612010 - 1596270\iota}) \\ &\approx (-3 - 3\iota, -26143.001822 + 4396.260260\iota), \\ (x_3, y_3) &= (1 + 2\iota, 10\sqrt{-1744002 + 734019\iota}) \\ &\approx (1 + 2\iota, 2721.885087 + 13483.651524\iota), \\ (x_4, y_4) &= (6 + 4\iota, -4\sqrt{99702405 - 110095815\iota}) \\ &\approx (6 + 4\iota, -44563.130818 + 19764.466810\iota). \end{aligned}$$

Using fig. 2 and the sequence of signs on Sheet 1, we identify that, y_1, y_2, y_4 are located on this sheet, and y_3 is located on the other sheet. Then we compute

$$\begin{aligned} \mathcal{A}(x_1, y_1) &= \mathcal{A}_{0,1} + \sum_{i=1}^2 \mathcal{A}_{i,i+1} - \int_{e_3}^{x_1} du, \\ \mathcal{A}(x_2, y_2) &= \mathcal{A}_{0,1} + \sum_{i=1}^3 \mathcal{A}_{i,i+1} + \int_{e_4}^{x_2} du, \\ \mathcal{A}(x_3, y_3) &= -\left(\sum_{i=1}^5 \mathcal{A}_{i,i+1} - \int_{e_6}^{x_3} du \right), \\ \mathcal{A}(x_4, y_4) &= \mathcal{A}_{0,1} + \sum_{i=1}^6 \mathcal{A}_{i,i+1} + \int_{e_7}^{x_4} du, \end{aligned}$$

and find

$$u(D) = \sum_{i=1}^4 \mathcal{A}(x_i, y_i) \approx \begin{pmatrix} -1.181275 + 0.204397\iota \\ 0.0736446 - 0.0379656\iota \\ -0.00480803 + 0.00259696\iota \\ 0.000610581 - 0.0000580815\iota \end{pmatrix}.$$

By means of (9) we compute

$$(31) \quad \begin{aligned} \wp_{1,1}(u(D)) &\approx -5 + 4\iota, & \wp_{1,1,1}(u(D)) &\approx 105.080464 - 182.470785\iota, \\ \wp_{1,3}(u(D)) &\approx 44 + 46\iota, & \wp_{1,1,3}(u(D)) &\approx -106.944505 - 1805.409841\iota, \\ \wp_{1,5}(u(D)) &\approx 122 + 160\iota, & \wp_{1,1,5}(u(D)) &\approx -8629.209325 + 183.256579\iota, \\ \wp_{1,7}(u(D)) &\approx 444 - 432\iota, & \wp_{1,1,7}(u(D)) &\approx -2469.693892 - 16677.610190\iota. \end{aligned}$$

Next, we use the solution (12) of the Jacobi inversion problem to verify if the obtained Abel image correspond to the given divisor D on the curve, and at the same time to verify the compliance of the obtained periods with the curve. For the given curve of genus 4 this solution acquires the form

$$\begin{aligned} \mathcal{R}_8(x; u) &\equiv x^4 - x^3\wp_{1,1}(u) - x^2\wp_{1,3}(u) - x\wp_{1,5}(u) - \wp_{1,7}(u) = 0, \\ \mathcal{R}_9(x, y; u) &\equiv 2y + x^3\wp_{1,1,1}(u) + x^2\wp_{1,1,3}(u) + x\wp_{1,1,5}(u) + \wp_{1,1,7}(u) = 0. \end{aligned}$$

The two entire rational functions in x and y , namely \mathcal{R}_8 and \mathcal{R}_9 , which both vanish on D , can be obtained as determinants of the two matrices, respectively,

$$\begin{aligned} \mathcal{R}_8(D) &= \begin{pmatrix} 1 & x & x^2 & x^3 & x^4 \\ \{1 & x_i & x_i^2 & x_i^3 & x_i^4\}_{i=1}^4 \end{pmatrix}, \\ \mathcal{R}_9(D) &= \begin{pmatrix} 1 & x & x^2 & x^3 & y \\ \{1 & x_i & x_i^2 & x_i^3 & y_i\}_{i=1}^4 \end{pmatrix}. \end{aligned}$$

After a proper normalization, we obtain

$$(32a) \quad \mathcal{R}_8(x; u(D)) = x^4 + (5 - 4\iota)x^3 - (44 + 46\iota)x^2 - (122 + 160\iota)x - 444 + 432\iota,$$

$$(32b) \quad \begin{aligned} \mathcal{R}_9(x, y; u(D)) &= 2y + (105.080464 - 182.470785\iota)x^3 \\ &- (106.944505 + 1805.409841\iota)x^2 - (8629.209325 - 183.256579\iota)x \\ &- 2469.693892 - 16677.610190\iota, \end{aligned}$$

Coefficients of the two functions give values of \wp -functions on D , and coincide with (31) with accuracy of 10^{-14} .

4.2. Example 1b. Let the divisor D be slightly modified, by changing y_3 into the value on Sheet 1. That is

$$\begin{aligned} (x_3, y_3) &= (1 - 2\iota, 10\sqrt{-1744002 + 734019\iota}) \\ &\approx (1 + 2\iota, -2721.885087 - 13483.651524\iota). \end{aligned}$$

Then $\mathcal{A}(x_3, y_3)$ is computed with the opposite sign:

$$\mathcal{A}(x_3, y_3) = \sum_{i=1}^5 \mathcal{A}_{i,i+1} - \int_{e_6}^{x_3} du.$$

Thus,

$$u(D) = \sum_{i=1}^4 \mathcal{A}(x_i, y_i) \approx \begin{pmatrix} -1.573357 + 0.028306\iota \\ 0.073072 - 0.049682\iota \\ -0.003687 + 0.002362\iota \\ 0.000908 + 0.000127\iota \end{pmatrix}.$$

Values of $\wp_{1,2i-1}$, $i = 1, 2, 3, 4$, remain the same, within the accuracy. The new values of $\wp_{1,1,2i-1}$, are

$$(33) \quad \begin{aligned} \wp_{1,1,1}(u(D)) &\approx -53.695371 - 181.736787i, \\ \wp_{1,1,3}(u(D)) &\approx -1058.131520 - 1483.454182i, \\ \wp_{1,1,5}(u(D)) &\approx -3204.406992 + 5874.230708i, \\ \wp_{1,1,7}(u(D)) &\approx 11061.251791 + 25177.554460i. \end{aligned}$$

Evidently, \mathcal{R}_8 remains unchanged, since values of x_i are kept the same. The new function \mathcal{R}_9 acquires the form

$$\begin{aligned} \mathcal{R}_9(x, y; u(D)) &= 2y - (53.695371 + 181.736787i)x^3 \\ &\quad - (1058.131520 + 1483.454182i)x^2 - (3204.406992 - 5874.230708i)x \\ &\quad + 11061.251791 + 25177.554460i, \end{aligned}$$

and its coefficients coincide with the values (33) with accuracy of 10^{-14} .

5. PERIODS ON A TRIGONAL CURVE

5.1. Trigonal curves. A generic trigonal curve is defined by the equation

$$(34) \quad 0 = f(x, y) = -y^3 + y^2\mathcal{T}(x) + y\mathcal{Q}(x) + \mathcal{P}(x).$$

Let maximal degrees of polynomials \mathcal{P} , \mathcal{Q} , \mathcal{T} be as shown in the table below, then the genus g of such a curve is computed as follows

$$\begin{aligned} \text{Case 1: } & \deg \mathcal{P} = 3\mathfrak{m} + 1, \quad \deg \mathcal{Q} = 2\mathfrak{m}, \quad \deg \mathcal{T} = \mathfrak{m}, \quad g = 3\mathfrak{m}; \\ \text{Case 2: } & \deg \mathcal{P} = 3\mathfrak{m} + 2, \quad \deg \mathcal{Q} = 2\mathfrak{m} + 1, \quad \deg \mathcal{T} = \mathfrak{m}, \quad g = 3\mathfrak{m} + 1; \\ \text{Case 3: } & \deg \mathcal{P} = 3\mathfrak{m} + 3, \quad \deg \mathcal{Q} = 2\mathfrak{m} + 2, \quad \deg \mathcal{T} = \mathfrak{m} + 1, \quad g = 3\mathfrak{m} + 1. \end{aligned}$$

Note that $y^2\mathcal{T}(x)$ is eliminated by the map $y \mapsto \tilde{y} + \frac{1}{3}\mathcal{T}(x)$, which leads to

$$\begin{aligned} 0 &= f(x, y) = -\tilde{y}^3 + \tilde{\mathcal{Q}}(x)y + \tilde{\mathcal{P}}(x), \\ \tilde{\mathcal{Q}}(x) &= \mathcal{Q}(x) + \frac{1}{3}\mathcal{T}(x)^2, \\ \tilde{\mathcal{P}}(x) &= \mathcal{P}(x) + \frac{1}{3}\mathcal{Q}(x)\mathcal{T}(x) + \frac{2}{27}\mathcal{T}(x)^3. \end{aligned}$$

Then the discriminant of (34) is

$$(35) \quad \Delta(x) = \tilde{\mathcal{P}}(x)^2 - \frac{4}{27}\tilde{\mathcal{Q}}(x)^3.$$

where

$$(36) \quad \deg \Delta = \begin{cases} 6\mathfrak{m} + 2, & \text{Case 1;} \\ 6\mathfrak{m} + 4, & \text{Case 2;} \\ 6\mathfrak{m} + 6, & \text{Case 3.} \end{cases}$$

The degree of Δ shows the number of finite branch points $B_i = \{(e_i, h_i)\}$. In Case 3 a curve has $6\mathfrak{m} + 6$ branch points, all finite. In Cases 1 and 2 a curve has the indicated in (36) number of finite branch points, and a double branch point at infinity. Let ν_i be the ramification index of B_i . Each branch point is counted $\nu_i - 1$ times. We assume, that all finite branch points have the ramification index 2, and the branch point at infinity B_0 has $\nu_0 = 3$.

Cases 1 and 2 with $\mathcal{T}(x) \equiv 0$ represent (n, s) -curves, which serve as canonical forms of trigonal curves. In these cases, the genus is computed by the formula $g = \frac{1}{2}(n-1)(s-1)$, see [9]. Case 3 is obtained by a proper bi-rational transformation of

Case 2, thus the both cases have the same Weierstrass gap sequence \mathfrak{W} . Therefore, classification of trigonal curves is based on Cases 1 and 2. The corresponding gap sequences are (each set is supposed to be ordered ascendingly)

$$\begin{aligned} \text{Case 1} \quad \mathfrak{W} &= \{3i - 2 \mid i = 1, \dots, \mathfrak{m}\} \cup \{3i - 1 \mid i = 1, \dots, 2\mathfrak{m}\}; \\ \text{Case 2} \quad \mathfrak{W} &= \{3i - 1 \mid i = 1, \dots, \mathfrak{m}\} \cup \{3i - 2 \mid i = 1, \dots, 2\mathfrak{m} + 1\}. \end{aligned}$$

With the help of Sato weights the order relation is introduced in the space of monomials $y^j x^i$. The latter are used to construct the equation of a curve, and also canonical differentials. The ordered lists of monomials in the both cases are

$$(37a) \quad \text{Case 1: } \mathfrak{M} = \{1, x, \dots, x^{\mathfrak{m}-1}, x^{\mathfrak{m}}, y, x^{\mathfrak{m}+1}, yx, \dots, x^{2\mathfrak{m}-1}, yx^{\mathfrak{m}-1}, x^{2\mathfrak{m}}, yx^{\mathfrak{m}}, y^2, x^{2\mathfrak{m}+1}, yx^{\mathfrak{m}+1}, \{y^2 x^i, x^{2\mathfrak{m}+1+i}, yx^{\mathfrak{m}+1+i} \mid i \in \mathbb{N}\}\},$$

$$(37b) \quad \text{Case 2: } \mathfrak{M} = \{1, x, \dots, x^{\mathfrak{m}-1}, x^{\mathfrak{m}}, y, x^{\mathfrak{m}+1}, yx, \dots, x^{2\mathfrak{m}-1}, yx^{\mathfrak{m}-1}, x^{2\mathfrak{m}}, yx^{\mathfrak{m}}, x^{2\mathfrak{m}+1}, y^2, yx^{\mathfrak{m}+1}, x^{2\mathfrak{m}+2}, \{y^2 x^i, yx^{\mathfrak{m}+1+i}, x^{2\mathfrak{m}+2+i} \mid i \in \mathbb{N}\}\}.$$

5.2. Riemann surface. In what follows, we focus on the canonical forms of trigonal curves:

$$(38) \quad 0 = f(x, y) = -y^3 + y\mathcal{Q}(x) + \mathcal{P}(x).$$

with the discriminant polynomial

$$\Delta(x) = \mathcal{P}(x)^2 - \frac{4}{27}\mathcal{Q}(x)^3.$$

Suppose that all roots of Δ are distinct, also \mathcal{P} and \mathcal{Q} have no common roots. These conditions are sufficient for the situation when the ramification index of every finite branch point is 2.

Solutions of (38) are given by the formula

$$(39a) \quad \begin{aligned} y_{+,a}(x) &= q_{+,a}(x) + \frac{1}{3}\mathcal{Q}(x)q_{+,a}^{-1}(x), \quad a = 1, 2, 3, \\ q_{+,a}(x) &= v_+^{1/3}(x)e^{2(a-1)\iota\pi/3}, \quad v_+(x) = \frac{1}{2}\left(\mathcal{P}(x) + \sqrt{\Delta(x)}\right), \end{aligned}$$

or equivalently

$$(39b) \quad \begin{aligned} y_{-,a}(x) &= q_{-,a}(x) + \frac{1}{3}\mathcal{Q}(x)q_{-,a}^{-1}(x), \quad a = 1, 2, 3, \\ q_{-,a}(x) &= v_-^{1/3}(x)e^{2(a-1)\iota\pi/3}, \quad v_-(x) = \frac{1}{2}\left(\mathcal{P}(x) - \sqrt{\Delta(x)}\right), \end{aligned}$$

where $\sqrt{\Delta}$ is defined by (21). By $q_{s,a}$, $s = \pm 1$, $a = 1, 2, 3$, three cubic roots of v_s are denoted. Let

$$(40) \quad v_s^{1/3}(x) = \begin{cases} |v_s(x)|^{1/3} e^{(\iota/3)\arg v_s(x)} & \text{if } \arg v_s(x) \geq 0, \\ |v_s(x)|^{1/3} e^{(\iota/3)\arg v_s(x) + \iota 2\pi/3} & \text{if } \arg v_s(x) < 0. \end{cases}$$

According to this definition, the function $v_s^{1/3}$ has the range $[0, \frac{2}{3}\pi)$, and its discontinuity is located over the contour $\Upsilon_s = \{x \mid \arg v_s(x) = 0\}$.

Theorem 2. *Let $v_s^{1/3}$ be defined by (40). Then each $y_{s,a}$ defined by (39) has a discontinuity on all three sheets over the contour $\Upsilon_s = \{x \mid \arg v_s(x) = 0\}$. Along a path from a region with $\arg v_s(x) < 0$ to a region with $\arg v_s(x) \geq 0$ the analytic continuation of $y_{s,a}$ is given by $y_{s,b}$, where $a \mapsto b$ according to the cyclic permutation (123).*

Proof. Let $s = +1$. Let \tilde{x} be located in the vicinity of the contour Υ_+ , more precisely $|\arg v_+(\tilde{x})| < 3\phi$, with a small positive value ϕ . Then $0 \leq \arg v_+^{1/3}(\tilde{x}) < \phi$ if $\arg v_+(\tilde{x}) \geq 0$, and $\frac{2}{3}\pi - \phi < \arg v_+^{1/3}(\tilde{x}) < \frac{2}{3}\pi$ if $v_+(\tilde{x}) < 0$. Therefore, Υ_+ is the contour of discontinuity of $v_+^{1/3}$.

Now, we find how the three values $q_{+,a}$ of $v_+^{1/3}$ are connected over Υ_+ . Let $U(x_0; \delta)$ be a disc of radius δ with the center at $x_0 \in \Upsilon_+$. The contour Υ_+ divides the disc into two parts: U_+ where $\arg v_+(x) \geq 0$, and U_- where $\arg v_+(x) < 0$. The analytic continuation of $v_+^{1/3}(x) = q_{+,1}(x)$ from U_+ to U_- is given by $e^{-\frac{2}{3}i\pi}v_+^{1/3}(x) = q_{+,3}(x)$, since $-\phi < \arg q_{+,3}(x) < 0$ if $x \in U_-$, and continuously connects to $q_{+,1}$ on U_+ . Similarly, the analytic continuation of $v_+^{1/3}(x) = q_{+,1}(x)$ from U_- to U_+ is given by $e^{\frac{2}{3}i\pi}v_+^{1/3}(x) = q_2(x)$. Therefore, along a path from U_- to U_+ , the function q_1 continuously connects to q_2 , then q_2 connects to q_3 , and q_3 connects to q_1 .

The same is true for $s = -1$. \square

Theorem 3. *Let $\sqrt{\Delta}$ be defined by (21). Then among three values of y , given by (39a), or (39b), two have discontinuity over the contour $\Gamma = \{x \mid \arg \Delta(x) = 0\}$. If Γ_i is a segment of Γ which starts at a branch point $B_i = (e_i, h_i)$, and $h_i = y_a(e_i) = y_b(e_i)$, then y_a, y_b are discontinuous over Γ_i , and y_a serves as the analytic continuation of y_b , and vice versa.*

Proof. According to Theorem 1, the both functions v_+, v_- , defined in (39), have discontinuity over the contour $\Gamma = \{x \mid \arg \Delta(x) = 0\}$, and serve the analytic continuation of each other. This implies that all $q_{s,a}$ have discontinuity over Γ , and for every a the analytic continuation of $q_{+,a}$ is given by $q_{-,a}$, and vice versa. We assume that $y_{+,a}$, $a = 1, 2, 3$, have discontinuity over Γ , which follows from the same property of $q_{+,a}$.

Recall the relation $v_+^{1/3}(x)v_-^{1/3}(x) = \frac{1}{3}e^{2ni\pi/3}\mathcal{Q}(x)$, where $n = 0, 1$, or 2 , such that $\arg v_+(x) + \arg v_-(x) = 3\arg \mathcal{Q}(x) + 2\pi n$ holds in the vicinity of x . This implies three equalities of the form $y_{+,a_1}(x) = y_{-,a_2}(x)$, where $a_1 \mapsto a_2$ according to one of the transpositions: (12), (13), or (23). Indeed,

$$\begin{aligned} n = 0 & \quad y_{+,1}(x) = y_{-,1}(x), \quad y_{+,2}(x) = y_{-,3}(x), \quad y_{+,3}(x) = y_{-,2}(x); \\ n = 1 & \quad y_{+,1}(x) = y_{-,3}(x), \quad y_{+,2}(x) = y_{-,2}(x), \quad y_{+,3}(x) = y_{-,1}(x); \\ n = 2 & \quad y_{+,1}(x) = y_{-,2}(x), \quad y_{+,2}(x) = y_{-,1}(x), \quad y_{+,3}(x) = y_{-,3}(x). \end{aligned}$$

Taking into account, that over Γ at every a the analytic continuation of $y_{+,a}$ is given by $y_{-,a}$, we see that among the three values of y given by (39a), or (39b), one remains continuous, and the other two serve as the analytic continuation of each other. Indeed, let $n = 0$ in the vicinity of x , then $y_{+,1}(x) = y_{-,1}(x)$. On the other hand, if a segment of Γ is located in this vicinity of x , then $y_{-,1}$ serves as the analytic continuation of $y_{+,1}$ over this segment, and so $y_{+,1}$ remains continuous. At the same time, $y_{-,2}(x) = y_{+,3}(x)$ serves as the analytic continuation of $y_{+,2}(x) = y_{-,3}(x)$, and vice versa, as follows from Theorem 1.

The contour Γ consists of segments Γ_i , each starts at e_i such that $B_i = (e_i, h_i)$ is a branch point. Let $x_0 \in \Gamma_i$ be located in the vicinity of e_i which does not contain Υ_+ , and $h_i = y_{+,a}(e_i) = y_{+,b}(e_i)$. Let $U(x_0, \delta)$ be a disc of radius δ centered at x_0 , such that $|x_0 - e_i| \geq \delta$. Then $U(x_0, \delta)$ is divided by Γ_i into two parts: U_+ where $\arg \Delta(x) \geq 0$, and U_- where $\arg \Delta(x) < 0$. There exists such c that $y_{+,c}(x) = y_{-,c}(x)$ for every $x \in U(x_0, \delta)$, and so $y_{+,c}$ is continuous over $U(x_0, \delta)$. Then a, b are

the other two values from $\{1, 2, 3\}$, since $y_{+,a}(x) = y_{-,b}(x)$ and $y_{+,b}(x) = y_{-,a}(x)$ over $U(x_0, \delta)$. Indeed, due to $\Delta(e_i) = 0$ we have $y_{+,a}(e_i) = y_{+,b}(e_i)$.

Similar considerations can be made in the case of $\mathbf{s} = -1$. \square

In what follows, we work with solutions $y_{+,a}$, $a = 1, 2, 3$, computed by the formula (39a), and denote them by y_a .

5.3. Homology. Let $\{B_i = (e_i, h_i)\}_{i=1}^N$ be branch points of a curve, sorted ascendingly first by $\operatorname{Re} e_i$, then by $\operatorname{Im} e_i$. The points are enumerated according to this order. Let all N finite branch points have the ramification index 2. A cut is made between two branch points, say B_i, B_j , at which the same sheets join. Note, that $N = 2(g+1)$ on canonical trigonal curves. Therefore, all branch points split into $g+1$ pairs connected by cuts. Let g cuts go through finite points, and the $(g+1)$ -th cut go through infinity. Cuts are made without intersection. Let $\{\mathfrak{a}_i\}_{i=1}^g$ encircle g finite cuts counter-clockwise. Let \mathfrak{b}_i come out from the $(g+1)$ -th cut, and enter the cut encircled by \mathfrak{a}_i .

5.4. Cohomology. First kind differentials are constructed with the help of the first g monomials from the ordered list \mathfrak{M} , namely:

$$(41) \quad du_{\mathfrak{w}_i} = \frac{\mathfrak{m}_{g-i+1}(x, y) dx}{\partial_y f(x, y)}, \quad i = 1, \dots, g,$$

where \mathfrak{m}_k is the k -th element of \mathfrak{M} , and $\mathfrak{w}_i \in \mathfrak{W}$.

A second kind differential $dr_{\mathfrak{w}_i}$, $\mathfrak{w}_i \in \mathfrak{W}$, is constructed with the help of the first $g+i$ monomials from \mathfrak{M} . Namely

$$(42) \quad du_{\mathfrak{w}_i} = \left(\sum_{j=1}^{g+i} c_{i,j} \mathfrak{m}_j(x, y) \right) \frac{dx}{\partial_y f(x, y)}, \quad i = 1, \dots, g.$$

The relation (7) defines the coefficients of monomials \mathfrak{m}_{g+i} , $i > 1$. Coefficients of the remaining part of the sum in (42) are also essential. In the case of trigonal curves, the second kind differentials associated to the standard first kind differentials (41) are obtained in [11] by means of the Klein formula.

5.5. Computation of periods. Based on the investigation presented in subsection 5.2, an algorithm of obtaining first kind periods on a canonical trigonal curve is developed. The curve is supposed to be generic, that is all finite branch points are single.

1. Find all finite branch points $\{B_i = (e_i, h_i)\}_{i=1}^N$ and pairs of analytical solutions y_a, y_b which join at each point, $h_i = y_a(e_i) = y_b(e_i)$. The point is labeled by 'a-b'. Let the branch points be sorted in the ascending order of real and imaginary parts. According to this order, a path through all branch points is constructed from straight line segments $[e_i, e_{i+1}]$, $i = 1, \dots, N$. Join the segment $(-\infty, e_1]$ at the beginning of the polygonal path, and $[e_N, \infty)$ at the end. See the path marked in orange on fig. 5. A path is chosen to be closed and homotopic to zero on each sheet of the curve.
2. Plot the contour $\Gamma = \{x \mid \arg \Delta(x) = 0\}$, see blue contours on fig. 5, and the contour $\Upsilon_+ = \{x \mid \arg v_+(x) = 0\}$, see green contours on fig. 5. Find

the sequence of changes of analytical solutions y_a , $a = 1, 2, 3$, on every sheet of the Riemann surface of the curve in question:

$$\begin{aligned} \text{Sheet 1:} & \quad \{\mathbf{a}_{0,1}\} \cup \{\mathbf{a}_{i,i+1}\}_{i=1}^{N-1} \cup \{\mathbf{a}_{N,0}\}, \\ \text{Sheet 2:} & \quad \{\mathbf{b}_{0,1}\} \cup \{\mathbf{b}_{i,i+1}\}_{i=1}^{N-1} \cup \{\mathbf{b}_{N,0}\}, \\ \text{Sheet 3:} & \quad \{\mathbf{c}_{0,1}\} \cup \{\mathbf{c}_{i,i+1}\}_{i=1}^{N-1} \cup \{\mathbf{c}_{N,0}\}. \end{aligned}$$

The sequence corresponds to the sequence of segments of the polygonal path, and takes into account intersections with Γ and Υ_+ . Index 0 is used for infinity.

3. Compute first kind integrals on each segment along the polygonal path:

$$(43a) \quad \mathcal{A}_{i,i+1}^{[n_{i,i+1}]} = \int_{B_i}^{B_{i+1}} du, \quad i = 1, \dots, N-1,$$

$$(43b) \quad \mathcal{A}_{0,1}^{[n_{0,1}]} = \int_{-\infty}^{B_1} du, \quad \mathcal{A}_{N,0}^{[n_{N,0}]} = \int_{B_N}^{\infty} du,$$

where $\mathbf{n} = \mathbf{a}, \mathbf{b}$, or \mathbf{c} , depending on the sheet. The integrand of $\mathcal{A}_{i,j}^{[n_{i,j}]}$ is defined by (41) with $y = y_{n_{i,j}}(x)$. If the chosen path is closed and homotopic to zero on each sheet, then

$$(44) \quad \mathcal{A}_{0,1}^{[n_{0,1}]} + \sum_{i=1}^{N-1} \mathcal{A}_{i,i+1}^{[n_{i,i+1}]} + \mathcal{A}_{N,0}^{[n_{N,0}]} = 0, \quad \mathbf{n} = \mathbf{a}, \mathbf{b}, \mathbf{c}.$$

The latter are used for verification.

4. Choose a basis of canonical cycles, and compute first kind period matrices ω , and ω' , then the normalized period matrix

$$\tau = \omega^{-1}\omega',$$

which is required to be symmetric with positive imaginary part.

5.6. Example 3: (3, 4)-curve. Consider the simplest trigonal curve in its canonical form

$$(45) \quad 0 = f(x, y) = -y^3 + x^4 + \lambda_2 y x^2 + \lambda_5 y x + \lambda_6 x^2 + \lambda_8 y + \lambda_9 x + \lambda_{12}.$$

From $\Delta(x) = 0$ we find x -coordinates e_i of branch points $B_i = (e_i, h_i)$. Then using (39a), we find the corresponding values of y_a , $a = 1, 2, 3$, two of which a, b coincide and give h_i . So each branch point is labeled by ' a - b ', that indicates which analytical solutions connect in the vicinity of this branch point.

A (3, 4)-curve possesses the gap sequence $\mathfrak{W} = \{1, 2, 5\}$, and the first kind differentials have the form

$$du = \begin{pmatrix} u_1 \\ u_2 \\ u_5 \end{pmatrix} = \begin{pmatrix} y \\ x \\ 1 \end{pmatrix} \frac{dx}{-3y^2 + \mathcal{Q}(x)}.$$

Let $\mathcal{A}_{i,j}^{[a]}$ denote the first kind integral between branch points B_i and B_j computed with the analytical solution $y = y_a(x)$, that is

$$(46) \quad \mathcal{A}_{i,j}^{[a]} = \int_{B_i}^{B_j} du(x, y_a(x)).$$

Second kind differential associated to the first ones on the curve (45) are defined as follows

$$dr = \begin{pmatrix} r_1 \\ r_2 \\ r_5 \end{pmatrix} = \begin{pmatrix} x^2 \\ 2xy \\ \mathcal{R}_5 \end{pmatrix} \frac{dx}{-3y^2 + \mathcal{Q}(x)},$$

$$\mathcal{R}_5 = 5x^2y + 3\lambda_3xy + \frac{2}{3}\lambda_2^2x^2 + \lambda_6y + \frac{2}{3}\lambda_2\lambda_5x.$$

As an example, we consider a curve defined by the equation

$$(47) \quad 0 = f(x, y) \equiv -y^3 + x^4 + y(4x^2 + 5x + 11) + 3x^3 + 7x^2 + 16x + 9.$$

The curve has eight finite branch points:

$e_1 \approx -4.58931,$	$h_1 \approx -4.9092$	2-3
$e_2 \approx -1.17922 - 0.934455i,$	$h_2 \approx 1.60505 + 0.430221i$	1-3
$e_3 \approx -1.17922 + 0.934455i,$	$h_3 \approx 1.60505 - 0.430221i$	1-3
$e_4 \approx -0.431732 - 2.20256i,$	$h_4 \approx 0.309255 - 1.83532i$	2-3
$e_5 \approx -0.431732 + 2.20256i,$	$h_5 \approx 0.309255 + 1.83532i$	1-2
$e_6 \approx 0.499118 - 1.57527i,$	$h_6 \approx -1.80047 + 1.31135i$	1-2
$e_7 \approx 0.499118 + 1.57527i,$	$h_7 \approx -1.80047 - 1.31135i$	2-3
$e_8 \approx 0.812986,$	$h_8 \approx -2.42959$	2-3

Fig. 5 displays the branch points and the contours where analytical solutions have discontinuities. The contour $\Upsilon_+ = \{x \mid \arg v_+(x) = 0\}$ is marked in green. Recall

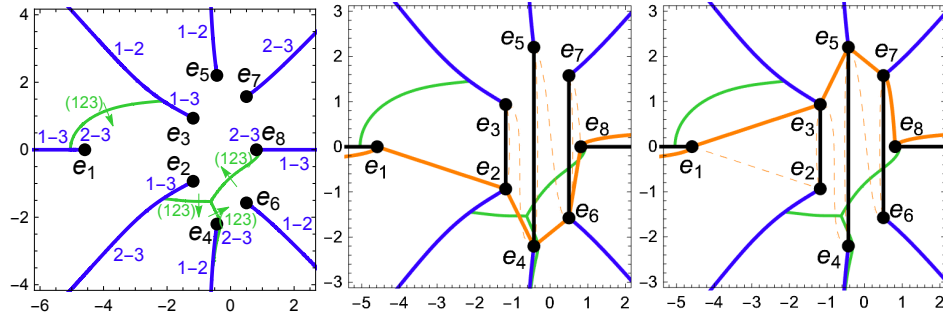


FIGURE 5. Contours Γ (blue), Υ_+ (green), cuts (black), and a path (orange).

that along Υ_+ all three solutions connect in pairs. Each segment of Υ_+ is labeled by the cyclic permutation (123) of analytical solutions, and an arrow shows in which direction this permutation occurs.

The contour $\Gamma = \{x \mid \arg \Delta(x) = 0\}$ is marked in blue. Segments $(-\infty, e_1]$ and $[e_8, \infty)$ also belong to Γ . Each segment Γ_i of Γ is labeled by a pair ‘ a - b ’ in the vicinity of the corresponding branch point $B_i = (e_i, h_i)$, where $h_i = y_a(e_i) = y_b(e_i)$. If Υ_+ intersects Γ_i , then the remaining part of Γ_i is labeled by another ‘ b - c ’ such that $y_b(x) = y_c(x)$ for all $x \in \Gamma_i$ after the intersection with Υ_+ away from the branch point. Fig. 5 reflects the density plots of y_a , $a = 1, 2, 3$, shown on fig. 6.

Cuts connect pairs of points: B_2 to B_3 along the sheets with analytic solutions y_1 and y_3 , B_4 to B_5 along the sheets with analytic solutions y_1 and y_2 in the vicinity

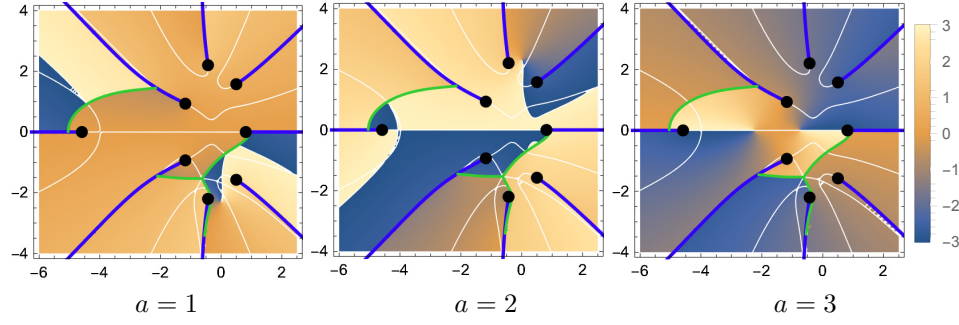


FIGURE 6. Density plot of $\arg y_{+,a}$, contours Γ (blue), Υ_+ (green).

of B_5 which change consequently into the pair 1–3 and then 2–3 when approaching B_4 , and B_6 to B_7 along sheets with analytic solutions y_1 and y_2 in the vicinity of B_6 which change into the pair 2–3 when approaching B_7 .

Let a path through all branch points be

$$\begin{aligned} &(-\infty, e_1] \cup [e_1, e_2] \cup [e_2, e_3] \cup [e_3, e_4] \cup [e_4, e_5] \\ &\cup [e_5, e_6] \cup [e_6, e_7] \cup [e_7, e_8] \cup [e_8, \infty), \end{aligned}$$

as shown on fig. 5 in orange. The path is polygonal, and is formed by straight lines between pairs of branch points. Every cut is rounded in counter-clockwise direction, as well as every branch point. In fact, the reader may see two variations of the path: (i) when the path goes on the right side of cuts, and (ii) on the left side. Each variation of the path can be continuously deformed into a simpler path. The full path is dashed, and simpler ones are solid.

In what follows we work with the path (i), which defines how analytical solutions (39a) connect along, determines sequences which represent each sheet:

$$\begin{aligned} \text{sheet 1: } &\{1, 1, 3, 3-1, 1-2-3, 3-2, 1-2, 2, 3\}, \\ \text{sheet 2: } &\{2, 2, 2, 2-3, 2-3-1, 1-3, 3-1, 1, 1\}, \\ \text{sheet 3: } &\{3, 3, 1, 1-2, 3-1-2, 2-1, 2-3, 3, 2\}. \end{aligned}$$

The indicated path is closed and homotopic to zero on each sheet, since the sum of first kind integrals along the path vanishes on each sheet. With a simplified path the following relations are obtained

$$\begin{aligned} (48) \quad &\mathcal{A}_{\infty-z\epsilon,1}^{[1]} + \mathcal{A}_{1,2}^{[1]} + \mathcal{A}_{2,4}^{[3-1]} + \mathcal{A}_{4,6}^{[1-2]} + \mathcal{A}_{6,8}^{[1-2]} + \mathcal{A}_{8,\infty+z\epsilon}^{[3]} = 0, \\ &\mathcal{A}_{\infty-z\epsilon,1}^{[2]} + \mathcal{A}_{1,2}^{[2]} + \mathcal{A}_{2,4}^{[2-3]} + \mathcal{A}_{4,6}^{[2-3]} + \mathcal{A}_{6,8}^{[3-1]} + \mathcal{A}_{8,\infty+z\epsilon}^{[1]} = 0, \\ &\mathcal{A}_{\infty-z\epsilon,1}^{[3]} + \mathcal{A}_{1,2}^{[3]} + \mathcal{A}_{2,4}^{[1-2]} + \mathcal{A}_{4,6}^{[3-1]} + \mathcal{A}_{6,8}^{[2-3]} + \mathcal{A}_{8,\infty+z\epsilon}^{[2]} = 0, \end{aligned}$$

where the superscript of $\mathcal{A}_{i,j}^{[a-b]}$ indicates that along the segment $[e_i, e_j]$ the analytic solution y_a connects to y_b over Υ_+ .

Note, that the three finite cuts are reachable on Sheet 3. Let \mathbf{a} -cycles be located on Sheet 3, encircling the three finite cuts. Let \mathbf{b}_i -cycle come out from the cut between e_1 and e_8 through infinity, and enter the cut encircled by \mathbf{a}_i -cycle, see fig. 7. Thus, periods are computed as follows

$$\omega_1 = \mathcal{A}_{2,3}^{[1]} + \mathcal{A}_{3,2}^{[3]},$$

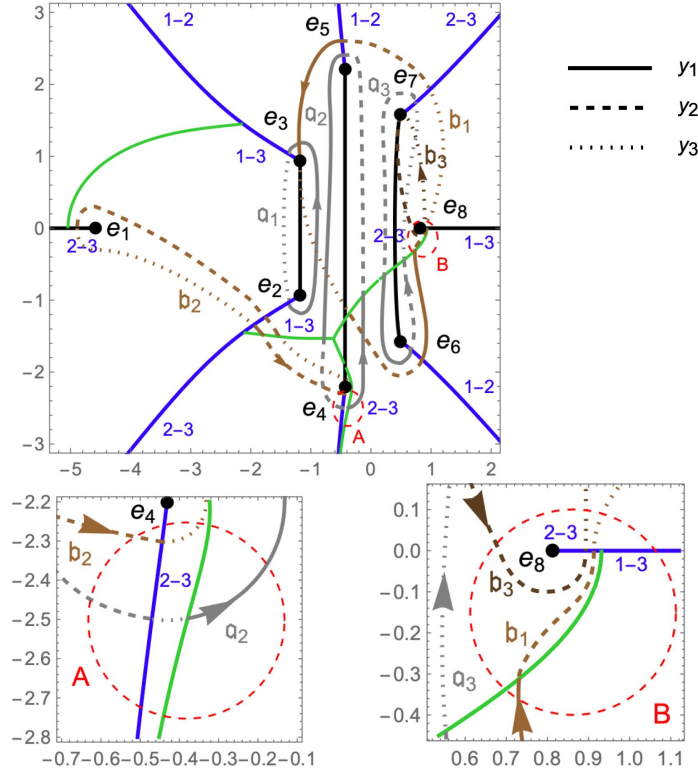


FIGURE 7. Cycles.

$$\begin{aligned}
 \omega_2 &= \mathcal{A}_{4,5}^{[3-1-2]} + \mathcal{A}_{5,4}^{[1-3-2]} = \mathcal{A}_{4,6}^{[3-1]} + \mathcal{A}_{6,5}^{[1-2]} + \mathcal{A}_{5,2}^{[1]} + \mathcal{A}_{2,4}^{[1-2]}, \\
 \omega_3 &= \mathcal{A}_{6,7}^{[2-3]} + \mathcal{A}_{7,6}^{[2-1]}, \\
 \omega'_1 &= \mathcal{A}_{8,7}^{[3]} + \mathcal{A}_{7,5}^{[2]} + \mathcal{A}_{5,3}^{[1]} + \mathcal{A}_{3,6}^{[3-2]} + \mathcal{A}_{6,8}^{[1-2]}, \\
 \omega'_2 &= \mathcal{A}_{1,2}^{[3]} + \mathcal{A}_{2,4}^{[1-2]} + \mathcal{A}_{4,2}^{[3-2]} + \mathcal{A}_{2,1}^{[2]}, \\
 \omega'_3 &= \mathcal{A}_{8,7}^{[3]} + \mathcal{A}_{7,8}^{[2]}.
 \end{aligned}$$

Computation gives the following not normalized period matrices

$$\begin{aligned}
 \omega &\approx \begin{pmatrix} -0.646716\iota & 1.367235\iota & -1.406214\iota \\ 0.557691\iota & 0.662524\iota & 0.237700\iota \\ -0.425220\iota & -0.085658\iota & 0.761823\iota \end{pmatrix}, \\
 \omega' &\approx \begin{pmatrix} 1.114221 + 0.360259\iota & -0.838244 + 0.360259\iota & 0.830310 - 0.703107\iota \\ -0.888801 + 0.610108\iota & -0.725076 + 0.610108\iota & -0.483530 + 0.118850\iota \\ 0.212490 - 0.255439\iota & 0.017209 - 0.255439\iota & -0.244951 + 0.380911\iota \end{pmatrix},
 \end{aligned}$$

and the normalized period matrix from the Siegel upper half-space

$$\tau \approx \begin{pmatrix} 0.5 + 1.204054\iota & 0.5 + 0.179707\iota & 0.413339\iota \\ 0.5 + 0.179707\iota & 0.5 + 0.879769\iota & 0.176635\iota \\ 0.413339\iota & 0.176635\iota & 0.5 + 0.572103\iota \end{pmatrix}.$$

Second kind period matrices are

$$\eta \approx \begin{pmatrix} -0.541959\iota & -0.385425\iota & -0.722057\iota \\ 1.52536\iota & -0.88414\iota & 0.484784\iota \\ 0.975636\iota & -1.01088\iota & -2.65892\iota \end{pmatrix},$$

$$\eta' \approx \begin{pmatrix} -1.357307 - 0.463692\iota & 2.945439 - 0.463692\iota & -0.354124 - 0.361028\iota \\ 2.292766 + 0.320609\iota & 5.356432 + 0.320609\iota & 2.131611 + 0.242392\iota \\ -5.584050 - 0.017623\iota & 4.038588 - 0.017623\iota & 6.689080 - 1.329459\iota \end{pmatrix},$$

and the symmetric matrix

$$\varkappa \approx \begin{pmatrix} 0.180731 & -0.994032 & -0.304044 \\ -0.994032 & 0.540116 & -1.367017 \\ -0.304044 & -1.367017 & -3.624898 \end{pmatrix}.$$

All computations are done in Wolfram Mathematica 12, with help of the function `NIntegrate`. With the `WorkingPrecision` of 18, the relations (48) hold with the accuracy 10^{-15} , as well as the symmetric property of τ . The symmetric property of \varkappa is satisfied up to 13 decimal digits.

6. COMPUTATION OF \wp -FUNCTIONS ON A TRIGONAL CURVE

First, the vector of Riemann constants should be defined, or its characteristic $[K]$. The theta function with characteristic $[K]$ possesses the maximal order of vanishing at $v = 0$, which is $(3\mathfrak{m} + 2)\mathfrak{m}$ on a $(3, 3\mathfrak{m} + 1)$ -curve, and $(3\mathfrak{m} + 4)\mathfrak{m}$ on a $(3, 3\mathfrak{m} + 2)$ -curve, due to the formula $\text{wgt } \sigma = -(n^2 - 1)(s^2 - 1)/24$.

Let $D = \sum_{i=1}^n (x_i, y_i)$ be a divisor on a curve. One should identify, to which sheet each point belongs, and compute the Abel image on the corresponding sheet, using the continuous path defined for this curve. Then \wp -functions are calculated by means of (9).

A solution of the Jacobi inversion problem, given by (13) or (14) on a canonical trigonal curve, can be used for computation of some \wp -functions. With a non-special degree g divisor, the two functions \mathcal{R}_{2g} , and \mathcal{R}_{2g+1} can be constructed as determinant of matrices constructed from the monomials in the list \mathfrak{M} .

Remark 4. The functions which arise as coefficients in this solution serve as a basis in the differential field of abelian functions on the curve, which means any other function can be expressed in terms of the basis functions.

6.1. Example 3. On the curve (45) with the homology basis chosen as shown on fig. 7 the characteristic of the vector of Riemann constants is

$$[K] = \begin{pmatrix} 1 & 0 & 1 \\ 0 & 1 & 1 \end{pmatrix},$$

and $\theta[K]$ vanishes to the order 5.

7. ACKNOWLEDGMENTS

The present paper was inspired by S. Matsutani, who expressed his interest to analytical computation of periods and \wp -functions in Mathematica.

REFERENCES

- [1] Agostini D., Chua L., Computing theta functions with Julia, *Journal of Software for Algebra and Geometry* **11** (2021), pp. 41–51
- [2] Baker H.F., *Abelian functions: Abel's theorem and the allied theory of theta functions*, Cambridge, University press, Cambridge, 1897.
- [3] Baker H.F., *Multiply periodic functions*, Cambridge Univ. Press, Cambridge, 1907.
- [4] Belokolos E. D., Bobenko A. I., Enolski V. Z., Its A. R., Matveev. V.B., *Algebro-geometric approach to nonlinear integrable equations.*, Springer-Verhag, 1994
- [5] Bernatska J., General derivative Thomae formula for singular half-periods, *Lett. Math. Phys.* (2020) (published online) arXiv:1904.09333 [math.AG]
- [6] Bernatska J., Reality conditions for the KdV equation and exact quasi-periodic solutions in finite phase spaces, preprint, arXiv:2312.10859.
- [7] Bernatska J., Leykin D. Solution of the Jacobi inversion problem on non-hyperelliptic curves, *Lett. Math. Phys.* **113** 110 (2023); arXiv:2212.14492
- [8] Bolza O. Ueber die Reduction hyperelliptischer Integrale erster Ordnung und erster Gattung auf elliptische durch eine Transformation vierten Grades, *Math. Ann.* **28**:3 (1887) pp. 447–456.
- [9] Buchstaber V. M., Enolskii V. Z., Leykin D. V., *Rational analogs of abelian functions*, *Functional Analysis and Its Applications*, **33**:2 (1999) pp. 83–94.
- [10] Buchstaber V. M., Enolskii V. Z., and Leykin D. V., *Hyperelliptic Kleinian Functions and Applications*, preprint ESI 380 (1996), Vienna
- [11] Buchstaber V. M., Enolskii V. Z., Leykin D. V., Uniformization of Jacobi varieties of trigonal curves and nonlinear differential equations, *Functional Analysis and Its Applications* **34** (2000) pp. 159–171
- [12] Bernatska J., General derivative Thomae formula for singular half-periods, *Lett. in Math. Phys.* **110** (2020), pp. 2983–3014.
- [13] J. Bernatska, New generalisation of Jacobi derivative formula, *Ramanujan J.*, **58** (2022), pp. 319–368.
- [14] Deconinck B., van Hoeij M., Computing Riemann matrices of algebraic curves, *Physica D* **152–153** (2001), pp. 28–46
- [15] Deconinck B., Patterson M. S., Computing with plane algebraic curves and Riemann surfaces: The algorithms of the Maple package “Algcurves” in *Computational approach to Riemann surfaces* (Lect. Notes Math. Vol. 2013), eds. Bobenko A. I., Klein C., Berlin: Springer, 2011,
- [16] Dubrovin B. A., Theta functions and non-linear equations, *Russ. Math. Surv.* 36:2 (1981), pp. 11–80
- [17] Enolski V.Z., Richter P.H. Periods of hyperelliptic integrals expressed in terms of θ -constants by means of Thomae formulae. *Phil. Trans. London Math. Soc. A* (2008), **366**, pp.1005–1024
- [18] Fay J. D., *Theta functions on Riemann surfaces*, *Lectures Notes in Mathematics* (Berlin), vol. 352, Springer, 1973.
- [19] Frauendiener J., Klein C., Hyperelliptic theta-functions and spectral methods, *Journal of Computational and Applied Mathematics* **167** (2004), pp.193–218.
- [20] Frauendiener J., Klein C., Hyperelliptic theta-functions and spectral methods: KdV and KP solutions, *Lett. Math. Phys.* **76**, (2006) pp. 249–267.
- [21] Kalla C., Klein C., On the numerical evaluation of algebro-geometric solutions to integrable equations, *Nonlinearity*, **25** (2012), pp. 569–596.
- [22] Matsutani S., Previato E., An algebro-geometric model for the shape of supercoiled DNA, *Physica D*, (2022) **430**, 133073
- [23] Matsutani S., A graphical representation of hyperelliptic KdV solutions, arXiv:2310.14656